

Molecular Dynamics Simulation of Phosphorus Trichloride (PCl₃) and Phosphorus Triiodide (PI₃) Liquids by Using the Force-fields Derived from a Quantum Chemical Approach

H. Moghadam*, B. Ghalami-Choobar* and M. Shafaghat-Lonbar

Department of Chemistry, Faculty of Science, University of Guilan, P. O. Box: 19141, Rasht, Iran

(Received 27 July 2020, Accepted 12 April 2021)

In this study, phosphorus trichloride (PCl₃) and phosphorus triiodide (PI₃), as the condensed inorganic materials, were investigated based on the molecular dynamics simulation. To this purpose, molecular dynamics (MD) simulations were performed by applying force field parameters derived from a quantum chemistry approach. The potential energies were computed at the B3LYP/6-31+G(d) and B3LYP/dgdzvpd levels of theory for different configurations of PCl₃ and PI₃, respectively. To determine force field parameters, a four-site all-atom force field model was used to correlate the potential energy data. Therefore, the force field parameters were applied to perform the molecular dynamics simulations. The MD simulations were performed to obtain the atomic number density, enthalpy, heat capacity, and radial distribution function in the NPT and NVT ensembles for PCl₃ and PI₃ dimers. There is a good consistency between the experimental data and simulation results over a wide range of experimental conditions.

Keywords: Molecular dynamics simulation, Force-field parameters, DFT calculations, Phosphorus trichloride, Phosphorus triiodide

INTRODUCTION

Computer simulation as a standard tool to facilitate the interpretation of experimental data relates the microscopic details of a system (masses of the atoms, molecular interaction potential parameters, molecular geometry, *etc.*) to macroscopic properties of experimental interest (equilibrium thermodynamic properties, transport properties, structural order parameters, and so on) [1,2]. The choice of force field depends on the system under investigation. If the refined force field is used, there should be a balance between the accuracy level and refinement of the molecular model in different parts [3]. The most common forms of force fields involve harmonic bond stretching and angle bending, Fourier series for torsion energies, and Coulomb plus Lennard-Jones terms for intermolecular non-bonded interactions [4]. Recently, formulation of force fields has been performed based on

quantum chemistry calculations, while many previous simulations used just empirical force fields taken from experimental measurements [5]. Hermia *et al.* calculated potential energy for different configurations of dimethyl ether dimer at the MP2/6-31+G** level of theory. Their simulated results for the condensed phase were satisfactorily consistent with both their experimental counterparts and those derived from empirical potentials. In the liquid phase, dimethyl ether molecules form dimer clusters. These occur preferentially in a conformation where the two molecules lie in the same plane [6,7].

Morsali *et al.* calculated potential energy for rigid SbF₅ and SbCl₅ at the B3LYP/6-31+G(d) level of theory. They derived a simple six-site force field model to reproduce the results of density functional theory (DFT) calculations. Adjusted force field parameters were used in the molecular dynamics (MD) simulations to obtain density, internal energy, enthalpy, and radial distribution function. They found a good agreement between MD results and experimental data [8]. Kongsuk *et al.* calculated the

*Corresponding authors. E-mail: homa.moghadam2013@yahoo.com; b.ghalami@gmail.com

interaction energies of the CCl_4 dimer for 800 configuration points at the MP2/6-31G level and employed the data to construct a five-site model. Their Monte Carlo (MC) simulations could well reproduce the experimental radial distribution functions (RDFs) [9]. Yurieva *et al.* used B3LYP method in a dgdzvp full electron basis set and of the method including pseudo potential for iodine compounds. The full-electron basis generally gives better agreement for X-I bond lengths and reaction enthalpies of iodination of organic compounds and equally good agreement in calculations of the IR vibrations of the X-I bond length compared to the results of the pseudo potential. The full-electron basis also allows adequate calculations of the quadruple coupling constants of iodine atoms and is generally characterized by shorter computing times [10]. Abbaspour *et al.* calculated thermodynamic properties and infinite shear modulus of HFD-like fluid using the statistical mechanical formula for neon. They considered quantum corrections using the Feynman-Hibbs (FH) approach. Also, they showed that the quantum and three-body effects improve the prediction of the pressure and internal energy of the HFD-like fluid [11].

Considering the continuing interest in the structure of molecular fluids, especially in which their constituent molecules are highly symmetric with a well-defined shape, in our previous work. We constructed a DFT force field using a high level of quantum chemistry theory for 9 configurations of the PBr_3 dimer [12]. Phosphorus trichloride (PCl_3) is a chemical compound of phosphorus and chlorine, having the chemical formula of PCl_3 with molecular mass: 137.35, boiling point: 76°C and melting point: -93.6°C . PCl_3 is known as a precursor for PCl_5 , POCl_3 and PSCl_3 , which are used in many applications, including herbicides, insecticides, plasticizers, oil additives, and flame retardants. PCl_3 is the precursor to triphenylphosphine for the Wittig reaction, and phosphite esters which can be used as industrial intermediates, or used in the Horner-Wadsworth-Emmons reaction, both are important methods for making alkenes. It also can be used to make trioctylphosphine oxide (TOPO), used as an extraction agent, although TOPO is usually made up of corresponding phosphine. PCl_3 is also used as a reagent in organic synthesis. It is used to convert primary and secondary alcohols into alkyl chlorides, or carboxylic acids

into acyl chlorides, although thionyl chloride generally gives better yields than PCl_3 [13,14]. Phosphorus triiodide (PI_3) is a chemical compound of phosphorus and iodine, having the chemical formula of PI_3 , with molecular mass: 411.6872, boiling point: 200°C , and melting point: 61°C . Phosphorus triiodide (PI_3) is an unstable red solid which reacts violently with water. It is a common misconception that PI_3 is too unstable to be stored; it is, in fact, commercially available. It is widely used in organic chemistry for converting alcohols to alkyl iodides [13]. Phosphorus triiodide is commonly used in the laboratory for the conversion of primary or secondary alcohols to alkyl iodides [15]. However, the structure of PX_3 ($X = \text{Cl}, \text{Br}, \text{I}$) trigonal pyramidal shape molecular liquids have been investigated from X-ray diffraction, MD simulations, and reverse MC modeling by Pothoczki *et al.* [16]. However, due to the challenges of determining the empirical force field from experimental measurements [17,18] and continuation of our ongoing research on the molecular fluids with trigonal pyramidal shape [12], we report the results of our study on PCl_3 and PI_3 molecules based on a quantum chemistry calculation and MD simulations. The purpose of the present paper is to construct a four-site all-atom model using a high level of quantum theory for different configurations of the PCl_3 and PI_3 dimers. The intermolecular potentials are fitted with DFT calculations of PCl_3 and PI_3 dimers to determine the force field parameters. The MD simulations are performed to obtain the atomic number density, enthalpy, heat capacity, and RDFs in the NPT ensemble for PCl_3 and PI_3 dimers. Accuracy of the obtained force field parameters is determined through a comparison of MD simulation results and experimental data.

COMPUTATIONAL DETAILS

In this study, the quantum chemistry calculations were performed on PCl_3 and PI_3 molecules using the Gaussian 03 software package [19]. First, the geometries of isolated PCl_3 and PI_3 molecules were fully optimized using the 6-31+G(d) and dgdzvp basis sets at the B3LYP level of theory and were found to be at the trigonal pyramidal configuration with the P-Cl bond length of 2.084 \AA (in consistent with the experimental data 2.043 \AA) and the bond angle for Cl-P-Cl

is 100.5° (in consistent with the experimental data 100.1°) and also the P-I bond length of 2.424 \AA (in consistent with the experimental data 2.430 \AA) and the bond angle for I-P-I is 109.5° (in a rather consistent with the experimental data 102.0°) [20-22]. The 9 symmetric conformers were chosen to sample the orientation dependence for each molecule (PCl_3 and PI_3 dimers), as shown in Figs. 1 and 2.

Subsequently, the phosphor-phosphor distance, denoted as R , was sampled for a large range of $2\text{-}12 \text{ \AA}$, with 100 configuration points for each conformer. A total of 900 configuration points were actually sampled and the energies were calculated for each. During the scan, all molecules were considered rigid and the optimized structures of the monomer were used for their geometry. The MD simulations were performed by the MOLDY package [23]. MOLDY is a C program for performing MD simulations on solids and liquids containing atoms, molecules, or ions in any mixture using periodic boundary conditions (PBC). Also, MOLDY implements periodic boundary conditions and the link-cell method and uses quaternions to describe molecular orientations. It also uses the Ewald summation in the evaluation of coulombic interactions, and the link-cell algorithm for evaluation of the interactions. The real (r_c) and k-space (k_c) interaction cut-offs and Ewald parameter (α) were determined by using Eqs. ((1)-(4)):

$$E = \exp(-\rho) \quad (1)$$

$$r_c = \frac{\sqrt{\rho}}{\alpha} \quad (2)$$

$$k_c = 2\alpha\sqrt{\rho} \quad (3)$$

$$\alpha = \sqrt{\pi} \left(\frac{t_R}{t_F} \frac{N}{V^2} \right)^{\frac{1}{6}} \quad (4)$$

where N is the number of molecules, V is the volume of the cell and t_R/t_F has been empirically determined to be 5.5 for MOLDY. In this study, we used a typical box length of 8.5125 \AA (in a simulation of 1000 molecules of PCl_3 or PI_3 at 0.1 MPa), this gave $r_c = 2.5 \text{ \AA}$. The number of time steps and the size of time step were 50.000 and 0.001 ps . Each run was equilibrated for 50 ps (for temperature scaling, as

discussed below), and statistics were accumulated for 50 ps . Results were collected on a constant NPT ensemble. The pressure was kept constant using the method of Parrinello and Rahman, and all the off-diagonal components of the stress matrix were fixed to zero. During the equilibration phase, the temperature of the simulation was controlled by re-scaling the velocities for each time step by using Eq. (5):

$$S = \sqrt{\frac{gKBT}{2\langle K \rangle}} \quad (5)$$

where g is the degree of freedom, k_B is the Boltzmann constant, T is the desired temperature, and $\langle K \rangle$ is the rolling average of the system kinetic energy over the previous time steps. The scaling was carried out separately for translational and rotational components. The re-scaling was turned off once the temperature of the system reached the equilibrium about the desired value, in order to generate a realization of the constant NPT ensemble. During the unscaled runs, temperatures were constant [24].

In this study, MD calculations were performed to obtain density, internal energy, enthalpy, and RDF at 1 ATM using LJ potential. The PBC was applied for MD calculations as usual. The PBC were used to MD calculations as usual. The MD calculations were implemented for a system of 500, 1000, 1500, 2000, 2500, 3000 PCl_3 and PI_3 molecules in NPT ensemble, separately.

RESULTS AND DISCUSSIONS

DFT Calculations

DFT (B3LYP) method was used to calculate the potential energies of different configurations of monomers and dimers of PCl_3 and PI_3 . Figures 1 and 2 show different symmetric configurations of the PCl_3 and PI_3 dimers, respectively. The interaction energies (E_{total}) were obtained by using Eq. (6):

$$E_{\text{total}} = E_D - 2E_M \quad (6)$$

where E_D and E_M denote energies of dimer and monomer, respectively. Figure 3 represents the curves of E_{total} and potential energy, at the B3LYP/6-31+g(d) and

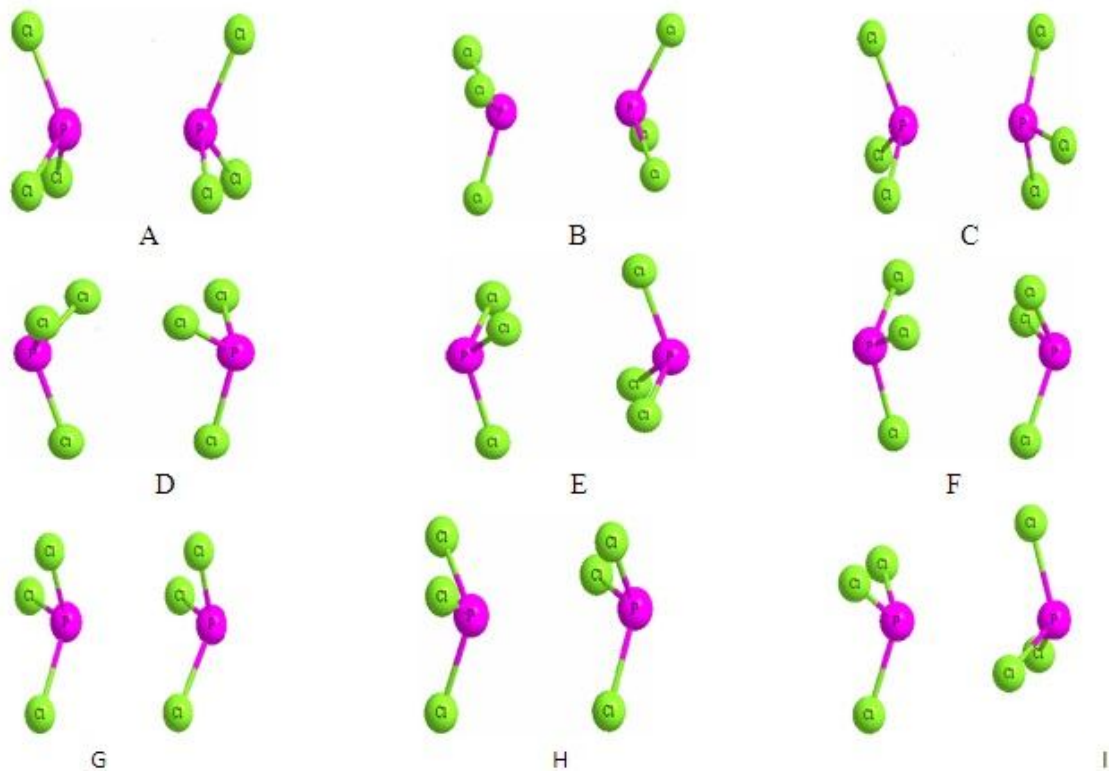


Fig. 1. The 9 symmetric conformers of the PCl_3 dimer (each conformer is shown by a capital letter from A to I).

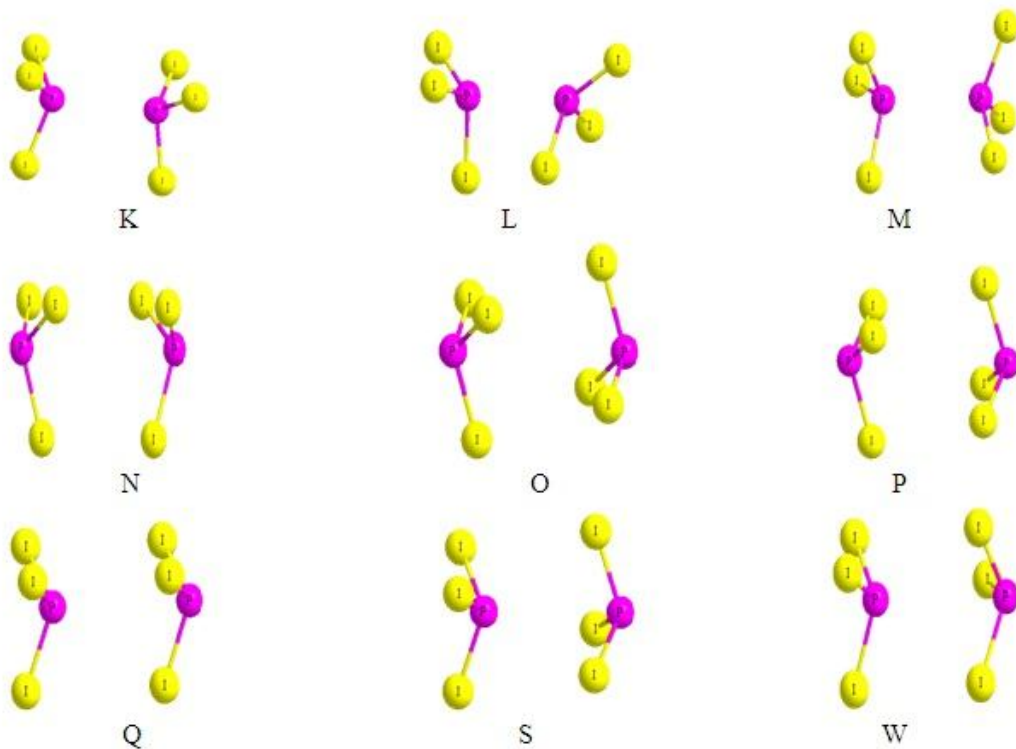


Fig. 2. The 9 symmetric conformers of the PI_3 dimer (each conformer is shown by a capital letter from K to W).

B3LYP/dgdzvp levels, for different symmetric configurations of the PCl_3 and PI_3 dimers, respectively.

Additionally, Tables S1 and S2, in Supporting Information, indicate the interaction energies. It can be seen that for the A-I conformers, the A, H and I, the B, C and G, and the F, E potential curves in Fig. 3a, and for the L-W conformers, the L and Q, the P and N, and the S and W potential curves in Fig. 3b are numerically identical, respectively. One of the most interesting issues in connection with the structure of the molecular liquids is how, and to what extent, the molecular shape determines the mutual orientations of molecules; *i.e.*, the orientational correlations. Furthermore, if the molecules possess permanent dipole moments, how dipolar interactions influence the short-range ordering. The competition (and therefore, eventually, a delicate balance) between electrostatic (dipolar) and steric effects, which can be different to each system, encouraged us to investigate a peculiar group of molecular liquids, namely the PX_3 ($X = \text{Cl}, \text{Br}, \text{I}$) family. As well, Tables 1 and 2 illustrate the partial charges and dipole moment (Debye) with several methods and different levels of theory for PCl_3 and PI_3 , respectively. The values of experimental dipole moments for PCl_3 and PI_3 are 0.7800 and 0.1407 Debye which were taken from the literature [25-28].

Four-site All-atom Force Field Model and Estimating Force Field Parameters

After the calculation of DFT-based potential energy, analytical four-site model was used to represent the DFT potential data. The total energy was determined from the nonbonding and torsion energy using Eq. (7):

$$E_{\text{total}} = E_{\text{non-bonding}} + E_{\text{torsional}} \quad (7)$$

where the non-bonded interactions ($E_{\text{non-bonding}}$) are represented by summing the Coulomb and Lennard-Jones terms according to Eq. (8) and torsional energies ($E_{\text{torsional}}$) were calculated from Eq. (9).

$$E_{\text{non-bonding}} = \sum_i \sum_j \left[\frac{q_i q_j e^2}{r_{ij}} + 4\epsilon_{ij} \left(\frac{\sigma_{ij}^{12}}{r_{ij}^{12}} - \frac{\sigma_{ij}^6}{r_{ij}^6} \right) \right] f_{ij} \quad (8)$$

$E_{\text{non-bonding}}$ is the potential energy of the system, i and j are

sites on atoms within the simulation cell, r_{ij} is the distance between sites i and j and q represents the atom charge, the summations in Eq. (8) are over the four interaction sites in both molecules. Where σ and ϵ are the diameter of the encounter and potential good depth, respectively. Moreover, $f_{ij} = 1.0$ except for intramolecular 1,4-interactions for which $f_{ij} = 0.5$. In addition, the torsion energy E_{torsion} is represented in Eq. (9).

$$E_{\text{torsion}}(\varphi) = \frac{V_1}{2}(1 + \cos(\varphi + f_1)) + \frac{V_2}{2}(1 - \cos(2\varphi + f_2)) + \frac{V_3}{2}(1 + \cos(3\varphi + f_3)) \quad (9)$$

where φ is the dihedral angle, V_1, V_2, V_3 are the coefficients in the Fourier series, f_1, f_2 and f_3 are phase angles, which are all zero for the present systems. In this model, $q_i, q_j, \sigma_{ij}, \epsilon_{ij}, V_1, V_2$ and V_3 are evaluated by using energy data in the fitting procedure [4]. We excepted some largest repulsive energy points from the fitting procedure to avoid their dominance in the least-squares cost function. The $q_i, q_j, \sigma_{ij}, \epsilon_{ij}, V_1, V_2$ and V_3 parameters were obtained by an iteration minimization procedure using the Microsoft Excel (solver) program. The obtained force field parameters are illustrated in Tables 3 and 4 for PCl_3 and PI_3 dimers, respectively. Standard combining rules were used such that $\sigma_{ij} = \frac{\sigma_i \sigma_j}{2}$ and $\epsilon_{ij} = (\epsilon_i \epsilon_j)^{0.5}$. The same expression was used for intramolecular non-bonded interactions between all pairs of atoms ($i < j$) separated by three or more bonds. Figure 4 shows a comparison of the DFT potential data using the 6-31+g(d) and dgdzvpd basis sets with fitting curves for each orientation of PCl_3 . Also, Fig. 5 shows a comparison of the DFT potential data using the dgdzvpd basis set with fitting curves for each orientation of PI_3 .

It can be observed that the electrostatic energies depend on orientation, leading to the relative stabilities for the configurations. Most potential data can be well represented by the fitting curves except those related to the repulsive energy data in the fitting procedure.

Molecular Dynamics Simulations

The obtained parameters were used to predict density, internal energy, enthalpy, and RDF in NPT ensemble for systems containing 500, 1000, 1500, 2000, 2500 PCl_3 and

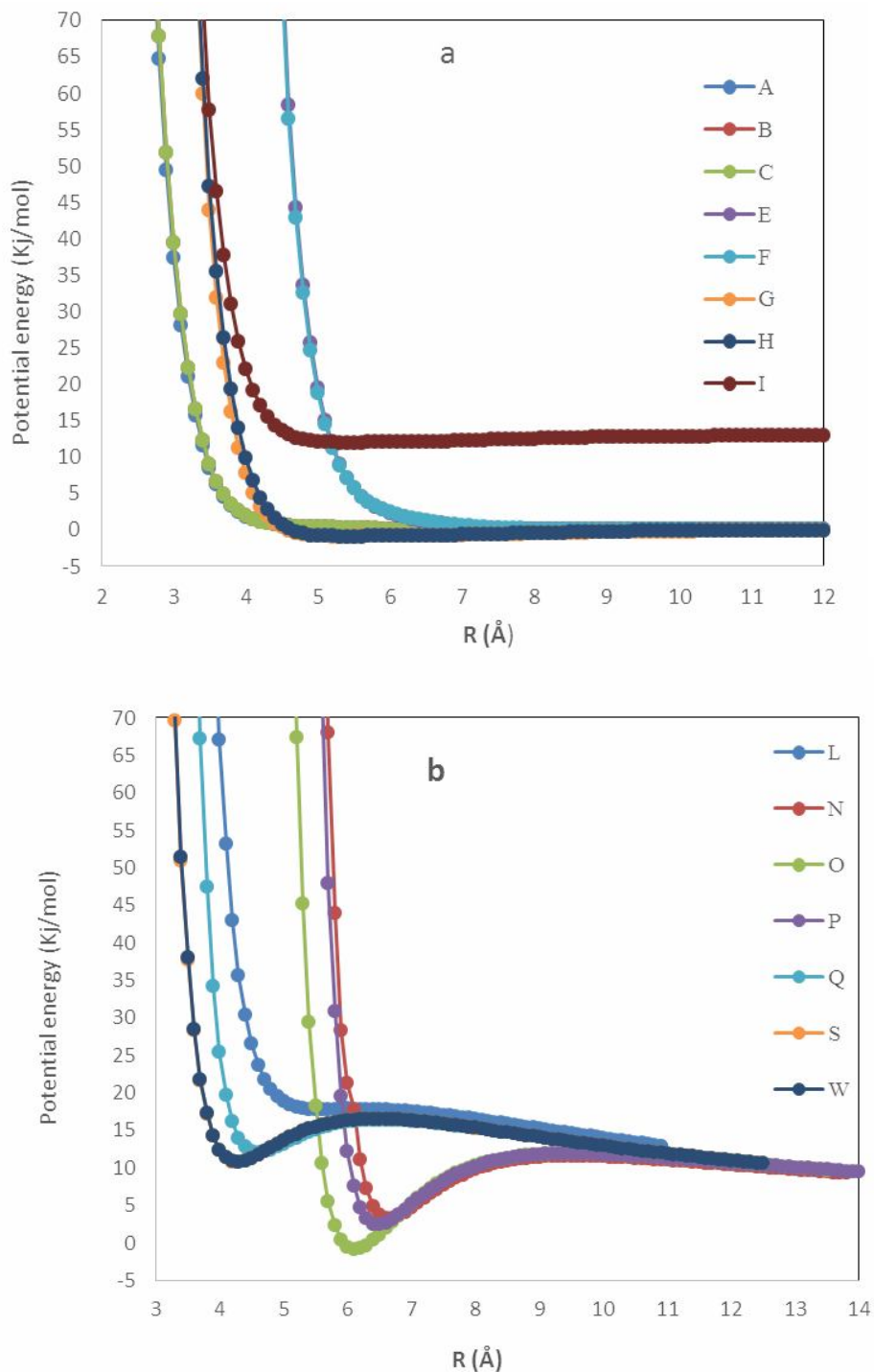


Fig. 3. (a) The curve of potential energy for different configurations of the PCI3 dimer at the B3LYP/6-31+G(d) level of theory (each conformer is shown by a capital letter from A to I) (b) The curve of E_{total} for different configurations of the PI3 dimer at the B3LYP/dgdzvpd level of theory.

Table 1. Partial Charges and Dipole Moment (Debye) with Several Methods and Different Levels of Theory for PCl_3

Level of theory	Method	Q_P (e)	Q_{Cl} (e)	Calculated dipole moment (Debye)	Literature Dipole moment (Debye)
HF/6-31+G	CHELPG	0.1857	-0.0619	0.6186	0.7800
B3lyp/6-31+G FOPT	Mulliken	0.2592	-0.0864	0.5844	0.7800
B3LYP/6-31+G	CHELPG	0.1754	-0.0585	0.5844	0.7800
B3LYP/6-31G**	CHELPG	0.0896	-0.0299	0.2985	0.7800
B3LYP/6-31G*	AIM	1.2080	-0.4030	0.7500	0.7800
B3lyp/6-31+G(d)	NBO	0.2419	-0.0806	0.3948	0.7800
RB3LYP/6-31+G(d)	Mulliken	0.2831	-0.0944	1.0465	0.7800
B3LYP/dgdzvp	Mulliken	0.5137	-0.1712	1.1258	0.7800
B3LYP/dgdzvp	CHELPG	0.2468	-0.0823	1.1258	0.7800
B3LYP/dgdzvp	NBO	0.5137	-0.1712	1.1258	0.7800
MP2/6-311+G(d)	Mulliken	-0.0962	0.0321	0.3359	0.7800
MP4/6-311+G(d)	Mulliken	-0.0962	0.0321	0.3359	0.7800
MP3/6-311+G(d)	Mulliken	-0.0962	0.0321	0.3359	0.7800
B3LYP/6-311++G	NBO	0.2419	-0.0801	0.3948	0.7800

Table 2. Partial Charges and Dipole Moment (Debye) with Several Methods and Different Levels of Theory for PI_3

Level of theory	Method	QP (e)	QI (e)	Calculated dipole moment (Debye)	Literature dipole moment (Debye)
HF/dgdzvp	NBO	0.4502	-0.1500	0.1407	0.1407
HF/SDD	NBO	-0.2236	0.0745	0.5868	0.1407
B3LYP/dgdzvp	NBO	0.3762	-0.1254	0.2806	0.1407
B3LYP/dgdzvp	Mulliken	0.3762	-0.1254	0.2806	0.1407
B3LYP/SDD	NBO	-0.0019	0.0006	0.4707	0.1407
B3LYP/SDD	Mulliken	-0.0019	0.0006	0.4707	0.1407
MP2/SDD	NBO	-0.2236	0.0745	0.5868	0.1407
Mp2/dgdzvp	NBO	0.4502	-0.1500	0.1407	0.1407
B3LYP/dgdzvp	Mulliken	0.4502	-0.1500	0.1407	0.1407
Mp3/dgdzvp	NBO	0.4502	-0.1500	0.1407	0.1407
RB3LYP/dgdzvp	NBO	0.3743	-0.1248	0.0412	0.1407
MP4/dgdzvp	Mulliken	0.4502	-0.1500	0.1407	0.1407

Table 3. The Force Field Parameters of PCl_3 Determined from Fitting Procedures

L-J parameters	ϵ (kJ mol ⁻¹)	σ (Å)	Dihedral parameters	
P-P	0.3515	3.7400	V1	0.0000
Cl-Cl	3.09528	3.0949	V2	2.0463
P-Cl	0.8894	3.5700	V3	0.0000

Table 4. The Force Field Parameters Determined of PI_3 from Fitting Procedures

L-J parameters	ϵ (kJ mol ⁻¹)	σ (Å)	Dihedral parameters	
P-P	0.4368	3.8600	V1	0.0000
I-I	2.9993	4.0776	V2	0.0000
P-I	0.6218	3.7050	V3	0.0000

PI_3 molecules at different temperatures by using the MOLDY package. We considered available thermodynamic conditions covering a density range of 1.337-1.989 g cm⁻³ and 3.584-4.045 g cm⁻³ at the temperature range of 178-400 K, and 273-600 K for PCl_3 and PI_3 , respectively. Table 5 shows the calculated densities for liquid PCl_3 from MD simulations and experimental data in the temperature range of 178-400 K. Also, the calculated densities for liquid PI_3 were illustrated in Table 6. Tables 5 and 6 show the densities obtained from MD calculations for different temperatures. As it is observed, there is a good consistency between the theoretical and experimental values, indicating that this simple model could be well used for predicting the PVT properties [29-32].

In Fig. 6, the RDFs calculated from molecular dynamics (MD) simulation in this work are compared with hard-sphere (HS), MD and reverse Monte Carlo (RMC) methods obtained by Pothoczki *et al.* [16].

The obtained results indicate that the RDFs are in better agreement with the hard-sphere model than other models.

The calculated peak positions of RDFs from this work were compared with the different methods in Tables 7 and 8. Table 9 is illustrated the MD values of the first maximum of $g_{pp}(r)$ for a number of different particles at a constant temperature.

The enthalpies (H) were also obtained based on the MD simulations at different temperatures and corresponding results were listed for PCl_3 and PI_3 in Tables 10 and 11, respectively. The heat capacities were obtained from the fitting of enthalpy values simulated at different temperatures. Furthermore, the obtained results were compared with reported data from the literature [28,29]. It can be seen that the obtained results are generally in good agreement with the literature data.

CONCLUSIONS

The quantum chemistry approach was used to obtain the potential energy for PCl_3 and PI_3 molecules. The potential energy was calculated at the B3LYP/6-31+G(d) and

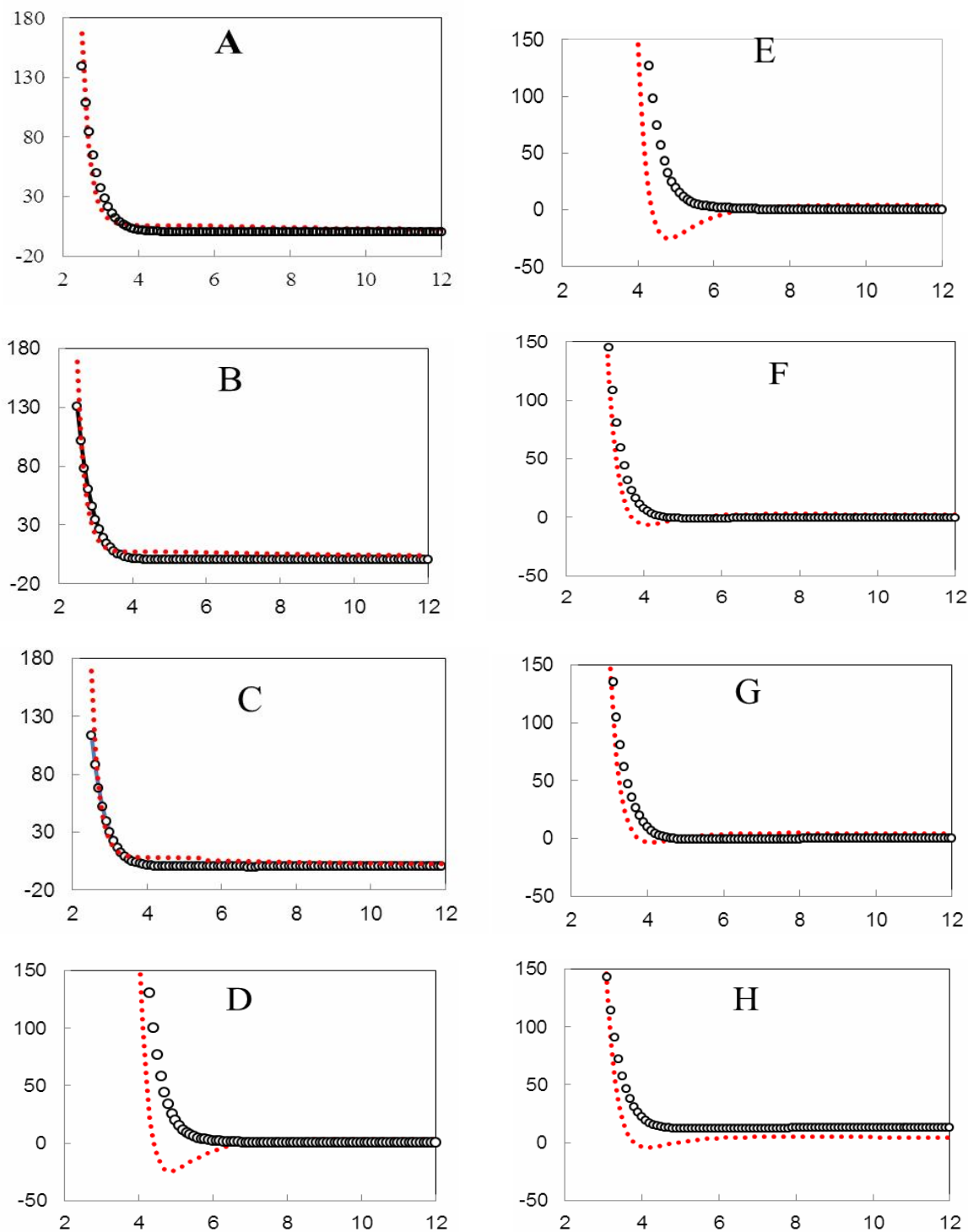


Fig. 4. Comparison of the representative fitting curves (dotted) and the potential data (o symbol) for each orientation of PCl₃ conformers (A-H) indicated in Fig. 1.

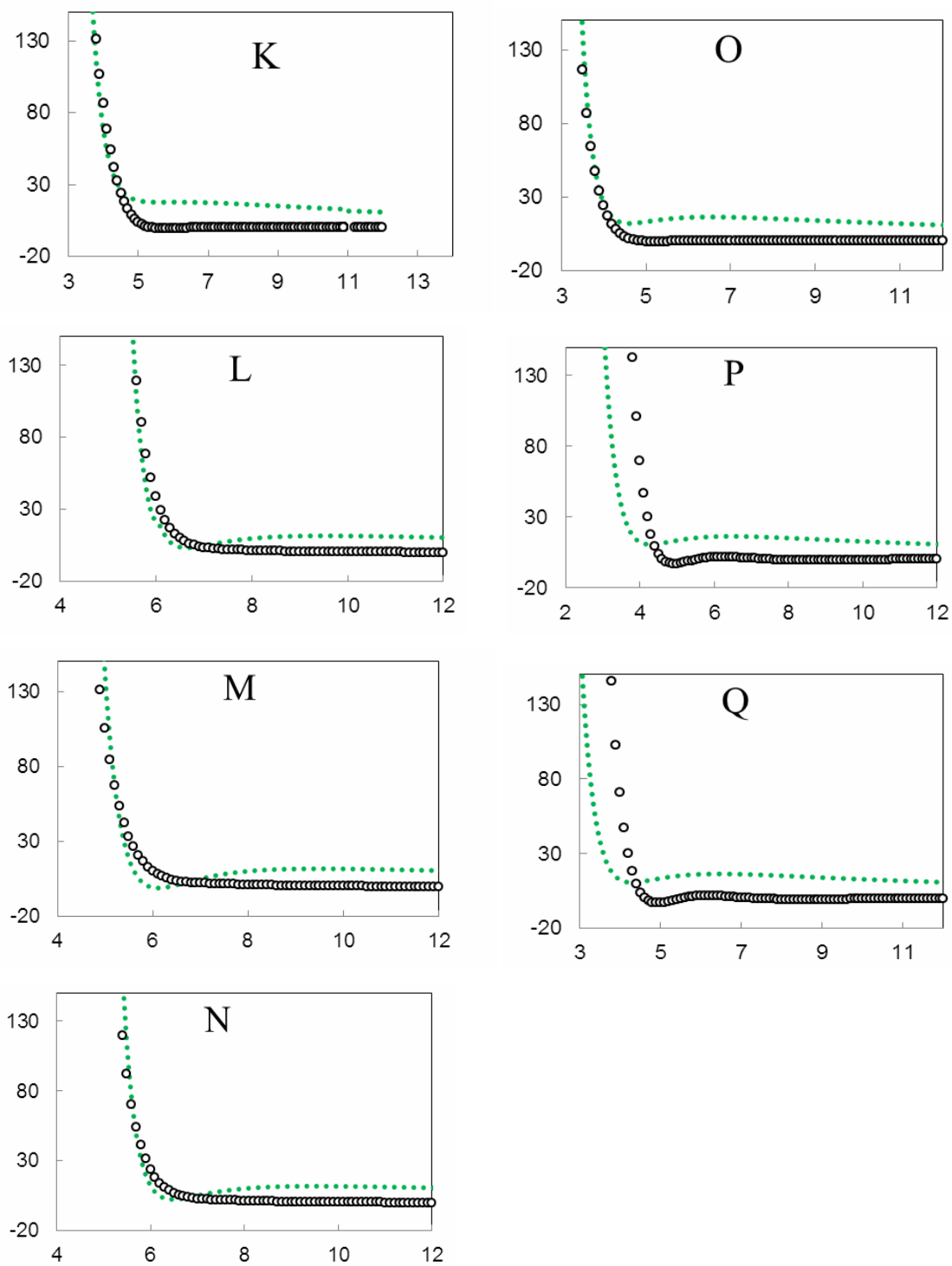


Fig. 5. Comparison of the representative fitting curves (dotted) and the potential data (● symbol) for each orientation of PI₃ conformers (K-Q) indicated in Fig. 2.

Table 5. Comparison of the Calculated and Experimental Data for PCl_3 Density in Various Temperatures ($n = 2000$ Molecules in Box)

T (K)	d_{cal} (g cm^{-3})	d_{exp} (g cm^{-3})
178	1.9893	1.7876
193	1.9451	1.7601
203	1.8977	1.7440
223	1.8640	1.7046
273	1.7154	1.6128
298	1.6394	1.5740
400	1.3369	1.4705

Table 6. Comparison of the Calculated and Experimental Data for PI_3 Density in Various Temperatures ($n = 2000$ Molecules in Box)

T (K)	d_{cal} (g cm^{-3})	d_{exp} (g cm^{-3})
273	4.0453	
293	4.0290	4.1800
333	3.9755	
473	3.7409	
600	3.5840	

Table 7. Comparison of the Calculated First Maximum Positions of the RDFs of PCl_3 with the Experimental Data from Ref. [16]

	$g_{\text{p-p}}(r)$	$g_{\text{p-cl}}(r)$	$g_{\text{cl-cl}}(r)$
MD	5.5	5.3	5.3
HS	5.5	5.3	3.2
RMC	5.5	5.3	6.4
MD _(this work)	5.6	5.2	3.1

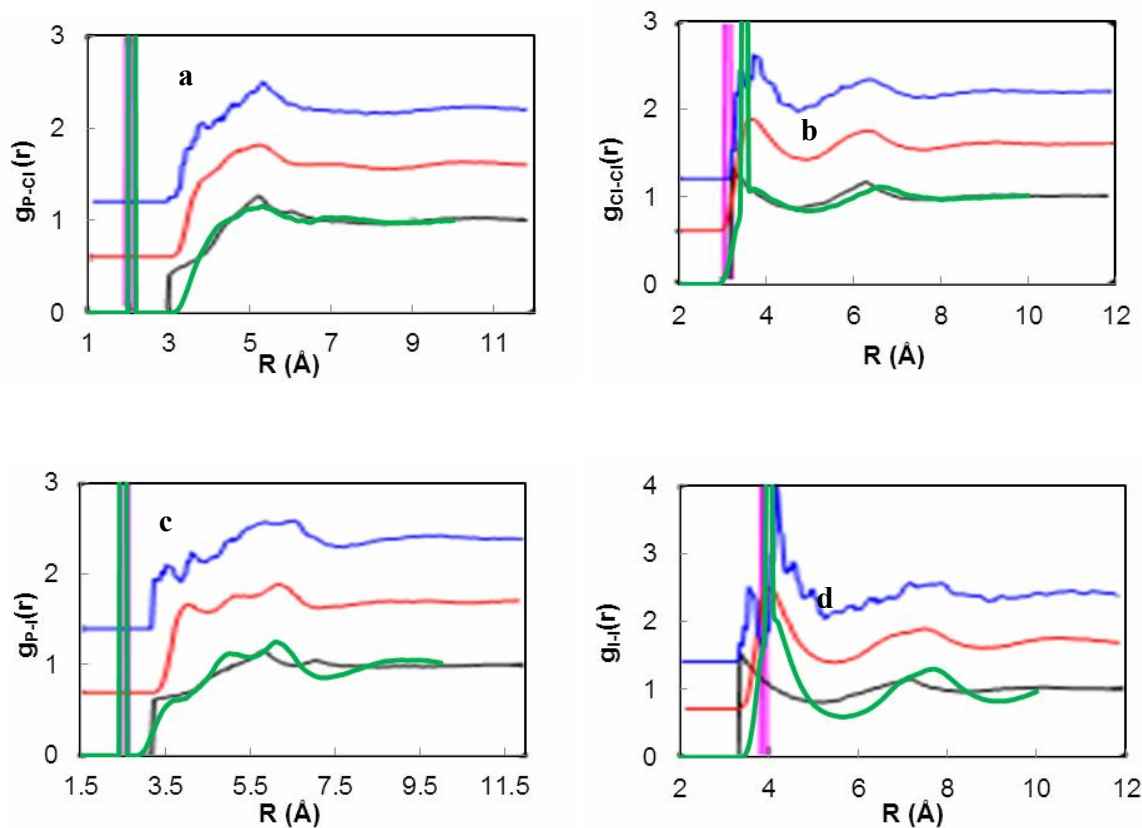


Fig. 6. The partial radial distribution functions $g(r)$ for PCl_3 and PI_3 (a) P-Cl, (b) Cl-Cl, (c) P-I and (d) I-I, Magenta line: intramolecular part for all models; black line: HS; red line: MD; blue line: RMC; (For interpretation of the references to [16]).

Table 8. Comparison of the Calculated First Maximum Positions of the RDFs of PI_3 with the Experimental Data from Ref. [16]

	$g_{\text{P-P}}(r)$	$g_{\text{P-I}}(r)$	$g_{\text{I-I}}(r)$
MD	5.8	4.8	3.6
HS	5.8	4.8	3.8
RMC	5.8	5.7	5.8
MD (this work)	5.6	4.9	3.9

B3LYP/dgdzvpd levels of theory for 9 configurations of PCl_3 and PI_3 dimers. The quantum chemistry derived potentials were used to determine force field parameters.

MD simulations were performed using force field parameters in the NPT ensemble for PCl_3 and PI_3 dimers. The density, internal energy, enthalpy, heat capacity and

Table 9. The First Maximum (MD) of $g_{p-p}(r)$ for PCl_3 and PI_3 at Constant Temperature 298 K and the Different Molecules Number in the Box

n	$g_{p-p}(r_{max}) (PCl_3)$	$g_{p-p}(r_{max}) (PI_3)$
500	2.8168	1.4462
1000	2.8505	1.3901
1500	2.3402	1.4400
2000	2.6574	1.4319
2500	2.3741	1.4163

Table 10. Comparison of the Calculated Enthalpy, and Heat Capacity for PCl_3 from MD Simulation Method with the Experimental Data

T (K)	$H_{simulation} (kJ mol^{-1})$	$C_p simulation (J mol^{-1} K^{-1})$	$C_p literature (J mol^{-1} K^{-1})$
178	-48779	70.17	65.60
193	-46583	70.32	69.56
203	-45313	70.42	71.81
223	-42422	70.62	75.59
273	-35043	71.12	
298.15	-31265	71.37	71.38
400	-17507	72.38	

Table 11. Values of the Calculated Enthalpy for PI_3 from MD Simulation Method

T (K)	$H_{simulation} (kJ mol^{-1})$
273	-66104
293	-65084
333	-63185
473	-55603
600	-49036

RDF were determined at different temperatures based on MD simulations and the results were compared with experiments. Quantitative agreements were observed between the observed RDFs, density, enthalpy and heat capacity with their experimental values for a wide range of thermodynamic conditions.

REFERENCES

- [1] Allen, M. P.; Tildesley, D. J., Computer Simulation of Liquids. 2356 Oxford University Press, **1987**.
- [2] van Gunsteren, W. F.; Dolenc, J.; Mark, A. E., Molecular simulation as an aid to experimentalists, *J. Curr. Opin. Struct. Biol.* **2008**, *2*, 149-153, DOI: 10.1016/j.sbi.2007.12.007.
- [3] Van Gunsteren, W. F.; Berendsen, H. J., Computer simulation of molecular dynamics: methodology, applications, and perspectives in chemistry, *J. Angew. Chem. Int. Ed. Engl.* **1990**, *29*, 992-1023, DOI: 10.1002/anie.199009921.
- [4] Jorgensen, W. L.; Maxwell, D. S., Development and testing of the OPLS all-atom force field on conformational energetics and properties of organic liquids, *J. Am. Chem. Soc.* **1996**, *118*, 11225-11236, DOI: 10.1021/ja9621760.
- [5] Wang, S. B.; Li, A. H. T.; Chao, S. D., Liquid properties of dimethyl ether from molecular dynamics simulations using ab initio force fields, *J. Comput. Chem.* **2012**, *33*, 998-1003, DOI: 10.1002/jcc.22930.
- [6] Hermida-Ramón, J.M.; Ríos, M.A., *Ab initio* molecular analysis of dimethyl ether dimer. Thermodynamic properties, *J. Theor. Chem.* **2000**, *105*(1), 1-6, DOI: 10.1007/s002140000173.
- [7] Hermida-Ramón, J. M.; Ríos, M. A., An *ab initio* polarizable intermolecular potential for dimethyl ether: application to liquid simulations, *J. Chem. Phys.* **2000**, *262*, 423-436, DOI: 10.1016/S0301-0104(00)00330-X.
- [8] Morsali, A.; Ghorbani, M.; Beyramabadi, S. A.; Bozorgmehr, M. R.; Heravi, M. M., A molecular dynamics study on the liquid SbCl₅ and SbF₅ using force fields derived from quantum chemical calculations, *J. Phys. Chem. Liq.* **2013**, *51*, 695-703, DOI: 10.1080/00319104.2013.782495.
- [9] Krongsuk, S.; Kerdcharoen, T.; Kiselev, M., Solvation structures of the 18-crown-6 in carbon tetrachloride as studied by Monte-Carlo simulation based on ab initio potential models, *J. Chem. Phys.* **2006**, *324*, 447-454, DOI: 10.1016/j.chemphys.2005.11.016.
- [10] Yurieva, A. G.; Poleshchuk, O. K.; Filimonov, V. D., Comparative analysis of a full-electron basis set and pseudopotential for the iodine atom in DFT quantum-chemical calculations of iodine-containing compounds, *J. Struct. Chem.* **2008**, *49*, 548-552, DOI: 10.1007/S 10948-008-0073-9.
- [11] Abbaspour, M.; A. Keyvanloo., Many-body and quantum effects in some thermodynamic properties and infinite shear modulus of HFD-like fluid using the radial distribution function, *J. Mol. Liq.* **2013**, *177*, 1-6, DOI: 10.1016/j.molliq.2012.09.023.
- [12] Ghalami-Choobar, B.; Moghadam, H.; Shafaghath-Lonbar, M., Molecular dynamics study on the liquid phosphorus tribromide by applying force-fields derived from quantum chemical approach, *J. Mol. Liq.* **2016**, *224*, 240-245, DOI: 10.1016/j.molliq.2016.09.078.
- [13] Muchmore, S. W.; Edmunds, J. J.; Stewart, K. D., Cheminformatic tools for medicinal chemists, *J. Med. Chem.* **2010**, *53*, 4830-4841, DOI: 10.1021/jm100164z.
- [14] Toy, A. D. F., Phosphorus, *Comprehensive Inorganic Chemistry*, **1973**.
- [15] Furniss, B. S.; Hannaford, A. J.; Smith, P. W. G.; Tatchell, A. R., Longman/Wiley, New York, **1989**.
- [16] Pothoczki, S.; Temleitner, L.; Pusztai, L., The structure of PX₃ (X = Cl, Br, I) molecular liquids from X-ray diffraction, molecular dynamics simulations, and reverse Monte Carlo modeling, *J. Chem. Phys.* **2014**, *140*, 054504, DOI: 10.1063/1.4863351.
- [17] Li, A. H. T.; Huang, S. C.; Chao, S. D., Molecular dynamics simulation of liquid carbon tetrachloride using ab initio force field, *J. Chem. Phys.* **2010**, *132*, 024506, DOI: 10.1063/1.3293129.
- [18] Chung, Y. H., Li, A. H. T. Chao, S. D., Computer simulation of trifluoromethane properties with *ab initio* force field, *J. Comput. Chem.* **2011**, *32*, 2414-2421, DOI: 10.1002/jcc.21823.

- [19] Lifang, X.; Yi, H., Construction of Gaussian03 parallel computing system based on AIX cluster, *J. Exp. Tech, Manage.* **2011**.
- [20] Kisliuk, P.; Townes, C. H., The microwave spectra and molecular structure of phosphorus and arsenic trichloride, *J. Chem. Phys.* **1950**, *18*, 1109-1110, DOI: 10.1063/1.1747872.
- [21] Hedberg, K.; Iwasaki, M., Effect of temperature on the structure of gaseous molecules. Molecular structure of PCl_3 at 300 and 505 K, *J. Chem. Phys.* **1962**, *36*, 589-594, DOI: 10.1063/1.1732575.
- [22] Denis, J. N.; Krief, A., Phosphorus tri-iodide (PI_3), a powerful deoxygenating agent, *J. Chem. Comm.* **1980**, *12*, 544-545, DOI: 10.1039/C39800000544.
- [23] Refson, K., MOLDY program can be downloaded from the internet at <http://www.ccp5.ac.uk/MOLDY/MOLDY.html> 2001.
- [24] Ackland, G. J.; D'Mellow, K.; Daraszewicz, S. L.; Hepburn, D. J.; Uhrin, M.; Stratford, K., The MOLDY short-range molecular dynamics package, *J. Comput. Phys. Commun.* **2011**, *182*, 2587-2604, DOI: 10.1016/j.cpc.2011.07.014.
- [25] Van Wazer, J. R., Phosphorus and its Compounds, **1958**.
- [26] Phosphorus Trichloride Available at www.inchem.org/documents/sids/sids/7719122.pdf
- [27] Phosphorus Trichloride, PCl_3 Available at phosphorus.atomistry.com/phosphorus_trichloride.html.
- [28] Chase Jr, M. W.; Davies, C. A.; Downey Jr, J. R.; Frurip, D. J; McDonald, R. A., Syverud, A. N., JANAF thermochemical tables (Third Edition), *J. Phys. Chem.* **1985**, *14*, 927-1856.
- [29] NIST chemistry webbook Available at <https://webbook.nist.gov>.
- [30] Li, A. H. T.; Huang, S. C.; Chao, S. D., Molecular dynamics simulation of liquid carbon tetrachloride using ab initio force field, *J. Chem. Phys.* **2010**, *132*, 024506, DOI: 10.1063/1.3293129.
- [31] Sherman, D. M.; Collings, M. D., Ion association in concentrated NaCl brines from ambient to supercritical conditions: results from classical molecular dynamics simulations, *J. Geochem. Trans.* **2002**, *3*, 102-107, DOI: 10.1039/b208671a.
- [32] Parrinello, M.; Rahman, A., Polymorphic transitions in single crystals: a new molecular dynamics method, *J. Appl. Phys.* **1981**, *52*, 7182, DOI: [org/10.1063/1.328693](https://doi.org/10.1063/1.328693).